

ELECTROMAGNETIC FORM FACTORS OF THE B MESON

By

MATTHEW DOMINIQUE MITCHELL

---

A Thesis Submitted to The Honors College  
In Partial Fulfillment of the Bachelors degree  
With Honors in  
Physics

THE UNIVERSITY OF ARIZONA

M A Y 2 0 1 9

Approved by:

---

Dr. Stefan Meinel  
Department of Physics

## Abstract

We provide a brief introduction to quantum field theories through the example of the Klein-Gordon scalar field both via canonical quantization and the path integral formulation. Next, we introduce the formalism of quantum chromodynamics, the quantum field theory of quarks and their interaction via the strong force. Here we demonstrate how to compute the quark field portion of  $n$ -point correlation functions and describe the lattice computation behind evaluating the remaining path integral over the gluon gauge field. In this thesis, we apply these methods to compute the  $b$  quark contribution to the electromagnetic form factor of the  $B$  meson. From the form factor, we extract the  $b$  quark contribution to the root mean square charge radius of the  $B$  meson and report this to be  $r_{\text{RMS}} = 0.349 \pm 0.95$  fm.

## Contents

<b>1</b>	<b>Introduction</b>	<b>2</b>
<b>2</b>	<b>Quantum Field Theory of a Scalar Field</b>	<b>2</b>
2.1	Canonical Quantization . . . . .	2
2.2	Path Integral Formulation . . . . .	5
<b>3</b>	<b>Quantum Chromodynamics</b>	<b>8</b>
3.1	Dirac Equation . . . . .	8
3.2	Quantum Chromodynamics and the Lattice . . . . .	8
3.2.1	Generating Functional and Contractions for the Dirac Field . . . . .	9
3.2.2	Computationally Solving the Gauge Field Path Integral . . . . .	10
<b>4</b>	<b>Electromagnetic Form Factor of the <math>B</math> Meson</b>	<b>11</b>
4.1	Electromagnetic Form Factors . . . . .	11
4.2	Computational Setup . . . . .	12
4.3	The $B$ Meson Form Factor . . . . .	12
4.3.1	Two-Point and Three-Point Correlation Functions for the $B$ Meson . . . . .	13
4.4	Results . . . . .	14
<b>5</b>	<b>Outlook</b>	<b>17</b>
	<b>References</b>	<b>17</b>

# 1 Introduction

The standard model of particle physics describes our natural world in terms of fundamental particles and four forces which govern their interactions. These forces are electromagnetism, the strong force, the weak force and gravity. There are six particles that interact via the strong force known as quarks which have six flavors, each of which has a quark and anti-quark, and are organized in to three generations of increasing mass. The two least massive quarks are the up ( $u$ ) and down ( $d$ ) quarks whose masses are on the order of 3 MeV. The next generation carries the charm ( $c$ ) and strange ( $s$ ) quarks which are about 100 times heavier than those of generation one. The last generation has the bottom ( $b$ ) quark, about 1,000 times heavier than generation one, and the top ( $t$ ) quark, about 10,000 times heavier than generation one. Because of the mass disparity between the quarks, generation one quarks are the most abundant and stable. Bound states of quarks are known as hadrons with some common examples being protons ( $uud$ ) and neutrons ( $udd$ ).

In this thesis, we're interested in the much less stable  $B$  meson ( $b\bar{u}$ ) and the  $b$  quark content of the electromagnetic form factor, which is the Fourier transform for the charge distribution. We begin with a discussion of quantum field theory, the mathematical foundations of the standard model. We consider two methods of quantization, the latter of which will become the foundation for a computational technique in quantum field theories. We then focus on a specific theory: quantum chromodynamics, the quantum field theory of the strong interaction. In this section we demonstrate how to compute correlation functions of quark fields in the interacting theory. Lastly, we derive the electromagnetic form factor for a particle, define it for the  $B$  meson and numerically calculate it as well as the root mean square  $b$  quark contribution to the charge radius of the  $B$  meson.

A theoretical computation of the  $B$  meson's form factor finds applications in providing a test of quantum field theory against experiment as well as other areas of theoretical physics. In [1], Elor et al. propose a mechanism that explains the relic abundance of dark matter and the matter/anti-matter asymmetry which explicitly depends on the  $B$  meson electromagnetic form factor. Currently, there are no experimental determinations of the  $B$  meson's form factor and the only theoretical values are from effective theories, e.g. [2], making a lattice computation of the  $B$  meson form factor rather important. Although our result, being only the  $b$  quark contribution to the form factor, can not be applied to this specific situation, it is a critical first step towards a full lattice calculation of the  $B$  meson form factor.

## 2 Quantum Field Theory of a Scalar Field

We begin by introducing the formalism behind quantum field theories through the example of the real Klein-Gordon scalar field. This provides a mathematical foundation for the formalism of quantum chromodynamics and our results on the form factor of the  $B$  meson to come. The material in this section has been heavily sourced from [3] and [4].

### 2.1 Canonical Quantization

The standard way to build a quantum field theory is known as canonical quantization. Because the process is highly dependent on the field we begin with, we work through a simple example, the real scalar Klein-Gordon field which has the Lagrangian density

$$\mathcal{L} = \frac{1}{2}(\dot{\phi})^2 - \frac{1}{2}|\nabla\phi|^2 - \frac{1}{2}m^2\phi^2. \tag{1}$$

Then the momentum density conjugate  $\pi$  to the field  $\phi$  is given by

$$\pi(\mathbf{x}) = \frac{\partial\mathcal{L}}{\partial\dot{\phi}(\mathbf{x})} = \dot{\phi}(\mathbf{x}). \tag{2}$$

We may now form the Hamiltonian density

$$\mathcal{H} = \pi(\mathbf{x})\dot{\phi}(\mathbf{x}) - \mathcal{L} = \frac{1}{2}\pi^2 + \frac{1}{2}(\nabla\phi)^2 + \frac{1}{2}m^2\phi^2. \tag{3}$$

This all comes from a classical field theory framework, to make this a quantum field theory we promote  $\phi$  and  $\pi$  to operators,  $\hat{\phi}$  and  $\hat{\pi}$ , indexed by the spatial coordinates. The operators are also, in general, depend on time, however, adopting the Heisenberg picture convention, we may always write any operator at some time  $t$  in terms of the zero-time operator evolved under the Heisenberg dynamics

$$\hat{\phi}(\mathbf{x}, t) = e^{-it\hat{H}}\hat{\phi}(\mathbf{x})e^{it\hat{H}}. \quad (4)$$

We now impose the canonical equal-time commutation relations

$$\begin{aligned} [\hat{\phi}(\mathbf{x}), \hat{\phi}(\mathbf{y})] &= [\hat{\pi}(\mathbf{x}), \hat{\pi}(\mathbf{y})] = 0 \\ [\hat{\phi}(\mathbf{x}), \hat{\pi}(\mathbf{y})] &= i\delta(\mathbf{x} - \mathbf{y}). \end{aligned} \quad (5)$$

The equation of motion for the classical Klein-Gordon field can be derived using the Euler-Lagrange equations and is given by

$$(\partial_t^2 - \nabla^2 + m^2)\phi(\mathbf{x}, t) = 0. \quad (6)$$

Applying the Fourier transform to this differential equation

$$(\partial_t^2 + \|\mathbf{p}\|^2 + m^2)\tilde{\phi}(\mathbf{p}, t) = 0 \quad (7)$$

we see that each mode behaves like an independent simple harmonic oscillator with  $\omega(\mathbf{p}) = \sqrt{\|\mathbf{p}\|^2 + m^2}$ . Recall the spectrum of the quantum mechanical simple harmonic oscillator can be easily discovered by the creation of the ladder operators. We expect that applying the same technique on the Klein-Gordon field will yield a similar result so we define the ladder operators in terms of the Fourier transforms of the operators  $\hat{\phi}$  and  $\hat{\pi}$  as

$$\hat{a}(\mathbf{p}) = \int \frac{d^3\mathbf{x}}{\sqrt{2\omega(\mathbf{p})}}(\omega(\mathbf{p})\hat{\phi}(\mathbf{x}) + i\hat{\pi}(\mathbf{x}))e^{-i\mathbf{x}\cdot\mathbf{p}} \quad (8)$$

$$\hat{a}^\dagger(\mathbf{p}) = \int \frac{d^3\mathbf{x}}{\sqrt{2\omega(\mathbf{p})}}(\omega(\mathbf{p})\hat{\phi}(\mathbf{x}) - i\hat{\pi}(\mathbf{x}))e^{i\mathbf{x}\cdot\mathbf{p}}. \quad (9)$$

The integrals in the above equation take care of Fourier transform and the difference in the signs in the exponent is chosen so that commutation relation between  $\hat{a}$  and  $\hat{a}^\dagger$  derived from (5) is as expected

$$\begin{aligned} [\hat{a}(\mathbf{p}), \hat{a}^\dagger(\mathbf{p}')] &= \int \frac{d^3\mathbf{x}d^3\mathbf{x}'}{2\sqrt{\omega(\mathbf{p})\omega(\mathbf{p}')}} \left[ (\omega(\mathbf{p})\hat{\phi}(\mathbf{x}) + i\hat{\pi}(\mathbf{x})) (\omega(\mathbf{p}')\hat{\phi}(\mathbf{x}') - i\hat{\pi}(\mathbf{x}')) \right. \\ &\quad \left. - (\omega(\mathbf{p}')\hat{\phi}(\mathbf{x}') + i\hat{\pi}(\mathbf{x}')) (\omega(\mathbf{p})\hat{\phi}(\mathbf{x}) - i\hat{\pi}(\mathbf{x})) \right] e^{-i(\mathbf{x}\cdot\mathbf{p} - \mathbf{x}'\cdot\mathbf{p}')} \\ &= \int \frac{d^3\mathbf{x}d^3\mathbf{x}'}{2\sqrt{\omega(\mathbf{p})\omega(\mathbf{p}')}} \left[ \omega(\mathbf{p})\omega(\mathbf{p}')([\hat{\phi}(\mathbf{x}), \hat{\phi}(\mathbf{x}')] + [\hat{\pi}(\mathbf{x}), \hat{\pi}(\mathbf{x}')]) \right. \\ &\quad \left. - i(\omega(\mathbf{p}') + \omega(\mathbf{p})) [\hat{\phi}(\mathbf{x}), \hat{\pi}(\mathbf{x}')] \right] e^{-i(\mathbf{x}\cdot\mathbf{p} - \mathbf{x}'\cdot\mathbf{p}')} \\ &= \frac{\omega(\mathbf{p}') + \omega(\mathbf{p})}{2\sqrt{\omega(\mathbf{p})\omega(\mathbf{p}')}} \int d^3\mathbf{x}d^3\mathbf{x}' \delta(\mathbf{x} - \mathbf{x}') e^{-i(\mathbf{x}\cdot\mathbf{p} - \mathbf{x}'\cdot\mathbf{p}')} \\ &= \frac{\omega(\mathbf{p}') + \omega(\mathbf{p})}{2\sqrt{\omega(\mathbf{p})\omega(\mathbf{p}')}} (2\pi)^3 \delta(\mathbf{p} - \mathbf{p}') \\ &= (2\pi)^3 \delta(\mathbf{p} - \mathbf{p}'). \end{aligned} \quad (10)$$

Now, solving for  $\hat{\phi}$  and  $\hat{\pi}$  in terms of the creation and annihilation operators

$$\hat{\phi}(\mathbf{x}) = \int \frac{d^3\mathbf{p}}{(2\pi)^3} \frac{1}{\sqrt{2\omega(\mathbf{p})}} (\hat{a}(\mathbf{p}) + \hat{a}^\dagger(-\mathbf{p})) e^{i\mathbf{x}\cdot\mathbf{p}} \quad \text{and} \quad (11)$$

$$\hat{\pi}(\mathbf{x}) = \int \frac{d^3\mathbf{p}}{(2\pi)^3} \sqrt{\frac{\omega(\mathbf{p})}{2}} (\hat{a}(\mathbf{p}) - \hat{a}^\dagger(-\mathbf{p})) e^{i\mathbf{x}\cdot\mathbf{p}}, \quad (12)$$

we can rewrite the Hamiltonian, the all-space integral of (3), as

$$\begin{aligned}
\hat{H} &= \int d^3\mathbf{x} \left( \frac{1}{2}\hat{\pi}^2(\mathbf{x}) + \frac{1}{2}(\nabla\hat{\phi}(\mathbf{x}))^2 + \frac{1}{2}m^2\hat{\phi}^2(\mathbf{x}) \right) \tag{13} \\
&= \int d^3\mathbf{x} \int \frac{d^3\mathbf{p}}{(2\pi)^3} \frac{d^3\mathbf{p}'}{(2\pi)^3} \left[ \frac{\sqrt{\omega(\mathbf{p})\omega(\mathbf{p}')}}{4} (\hat{a}(\mathbf{p}) - \hat{a}^\dagger(-\mathbf{p})) (\hat{a}(\mathbf{p}') - \hat{a}^\dagger(-\mathbf{p}')) \right. \\
&\quad \left. + \frac{m^2 - \mathbf{p} \cdot \mathbf{p}'}{4\sqrt{\omega(\mathbf{p})\omega(\mathbf{p}')}} (\hat{a}(\mathbf{p}) + \hat{a}^\dagger(-\mathbf{p})) (\hat{a}(\mathbf{p}') + \hat{a}^\dagger(-\mathbf{p}')) \right] e^{i\mathbf{x} \cdot (\mathbf{p} + \mathbf{p}')} \\
&= \int \frac{d^3\mathbf{p}}{(2\pi)^3} \frac{d^3\mathbf{p}'}{(2\pi)^3} \left[ \frac{\sqrt{\omega(\mathbf{p})\omega(\mathbf{p}')}}{4} (\hat{a}(\mathbf{p}) - \hat{a}^\dagger(-\mathbf{p})) (\hat{a}(\mathbf{p}') - \hat{a}^\dagger(-\mathbf{p}')) \right. \\
&\quad \left. + \frac{m^2 - \mathbf{p} \cdot \mathbf{p}'}{4\sqrt{\omega(\mathbf{p})\omega(\mathbf{p}')}} (\hat{a}(\mathbf{p}) + \hat{a}^\dagger(-\mathbf{p})) (\hat{a}(\mathbf{p}') + \hat{a}^\dagger(-\mathbf{p}')) \right] \delta(\mathbf{p} + \mathbf{p}') \\
&= \int \frac{d^3\mathbf{p}}{(2\pi)^3} \left[ \frac{\sqrt{\omega(\mathbf{p})\omega(-\mathbf{p})}}{4} (\hat{a}(\mathbf{p}) - \hat{a}^\dagger(-\mathbf{p})) (\hat{a}(-\mathbf{p}) - \hat{a}^\dagger(\mathbf{p})) \right. \\
&\quad \left. + \frac{|\mathbf{p}|^2 + m^2}{4\sqrt{\omega(\mathbf{p})\omega(-\mathbf{p})}} (\hat{a}(\mathbf{p}) + \hat{a}^\dagger(-\mathbf{p})) (\hat{a}(-\mathbf{p}) + \hat{a}^\dagger(\mathbf{p})) \right] \\
&= \int \frac{d^3\mathbf{p}}{(2\pi)^3} \frac{\omega(\mathbf{p})}{2} (\hat{a}(\mathbf{p})\hat{a}^\dagger(\mathbf{p}) + \hat{a}^\dagger(-\mathbf{p})\hat{a}(-\mathbf{p})) \\
&= \int \frac{d^3\mathbf{p}}{(2\pi)^3} \frac{\omega(\mathbf{p})}{2} (\hat{a}(\mathbf{p})\hat{a}^\dagger(\mathbf{p}) + \hat{a}^\dagger(\mathbf{p})\hat{a}(\mathbf{p})) \\
&= \int \frac{d^3\mathbf{p}}{(2\pi)^3} \omega(\mathbf{p}) \left( \hat{a}(\mathbf{p})\hat{a}^\dagger(\mathbf{p}) + \frac{1}{2} [\hat{a}(\mathbf{p}), \hat{a}^\dagger(\mathbf{p})] \right). \tag{14}
\end{aligned}$$

We notice that  $[\hat{a}(\mathbf{p}), \hat{a}^\dagger(\mathbf{p})] = (2\pi)^3\delta(0)$  is an infinity that results from the continuity of the spatial index  $\mathbf{x}$ . Were this a discrete system, this would be finite and the portion of the integral in (14)

$$\int \frac{d^3\mathbf{p}}{(2\pi)^3} \frac{\omega(\mathbf{p})}{2} [\hat{a}(\mathbf{p}), \hat{a}^\dagger(\mathbf{p})]$$

would correspond to the sum of the ground-state energies of all of the modes. This term just shifts all of the energy levels of the system by a constant and since only energy differences are physically measurable, for convenience we could always subtract this value out to normalize our ground-state energy to zero. Taking this idea to the continuum, this portion of the integral would disappear and we are left with

$$\hat{H} = \int \frac{d^3\mathbf{p}}{(2\pi)^3} \omega(\mathbf{p}) \hat{a}(\mathbf{p}) \hat{a}^\dagger(\mathbf{p}). \tag{15}$$

The process of removing this infinity from the Hamiltonian is an example of *renormalization* and it is still debated today whether this step is a fundamental hole in the logic of quantum field theories or if it is simply a necessary chore when constructing a quantum field theory. Lastly, we compute the commutator of the creation and annihilation operators with the Hamiltonian to show they behave just like the ladder operators for a simple harmonic oscillator

$$\begin{aligned}
[\hat{H}, \hat{a}^\dagger(\mathbf{p})] &= \int \frac{d^3\mathbf{p}'}{(2\pi)^3} \omega(\mathbf{p}') (\hat{a}(\mathbf{p}')\hat{a}^\dagger(\mathbf{p}')\hat{a}^\dagger(\mathbf{p}) - \hat{a}^\dagger(\mathbf{p})\hat{a}(\mathbf{p}')\hat{a}^\dagger(\mathbf{p}')) \\
&= \int \frac{d^3\mathbf{p}'}{(2\pi)^3} \omega(\mathbf{p}') [\hat{a}(\mathbf{p}'), \hat{a}^\dagger(\mathbf{p})] \hat{a}^\dagger(\mathbf{p}') \\
&= \int d^3\mathbf{p}' \delta(\mathbf{p} - \mathbf{p}') \omega(\mathbf{p}') \hat{a}^\dagger(\mathbf{p}') \\
&= \omega(\mathbf{p}) \hat{a}^\dagger(\mathbf{p}), \tag{16}
\end{aligned}$$

$$\begin{aligned}
[\hat{H}, \hat{a}(\mathbf{p})] &= \int \frac{d^3 \mathbf{p}'}{(2\pi)^3} \omega(\mathbf{p}') (\hat{a}(\mathbf{p}') \hat{a}^\dagger(\mathbf{p}') \hat{a}(\mathbf{p}) - \hat{a}(\mathbf{p}) \hat{a}(\mathbf{p}') \hat{a}^\dagger(\mathbf{p}')) \\
&= - \int \frac{d^3 \mathbf{p}'}{(2\pi)^3} \omega(\mathbf{p}') [\hat{a}(\mathbf{p}'), \hat{a}^\dagger(\mathbf{p}')] \hat{a}(\mathbf{p}') \\
&= - \int d^3 \mathbf{p}' \delta(\mathbf{p} - \mathbf{p}') \omega(\mathbf{p}') \hat{a}(\mathbf{p}') \\
&= -\omega(\mathbf{p}) \hat{a}(\mathbf{p}).
\end{aligned} \tag{17}$$

With this, we define the ground or vacuum state to be the state  $|0\rangle$  such that  $\hat{a}(\mathbf{p})|0\rangle = 0$  for all  $\mathbf{p} \in \mathbb{R}^3$ . This state has energy zero and we can build any energy state by applying the creation operator to the vacuum state any amount of times, i.e. the state  $\hat{a}^\dagger(\mathbf{p}_1) \cdots \hat{a}^\dagger(\mathbf{p}_n)|0\rangle$  has energy  $\omega(\mathbf{p}_1) + \cdots + \omega(\mathbf{p}_n)$ . As may have been explicit from the beginning due to the nomenclature, we can interpret these states as being multi-particle states, where each  $\hat{a}^\dagger(\mathbf{p})$  creates a particle with definite momentum  $\mathbf{p}$  and energy  $\omega(\mathbf{p}) = \sqrt{|\mathbf{p}|^2 + m^2}$ . Moreover, this energy formula exactly matches the energy of a particle predicted by special relativity.

## 2.2 Path Integral Formulation

Canonical quantization has no obvious computational counterpart and so we must devise a new, equivalent picture of quantum field theories that is more inclined to computation for situations where we fail to find analytical results. For this, we'll introduce the path integral formulation which allows us to compute transition amplitudes and correlation functions with integrals and thus has a clear computational counterpart in numerical integral techniques. Let's again consider the Klein-Gordon Lagrangian for simplicity. Let  $|\phi\rangle$  and  $|\pi\rangle$  for all functions  $\phi, \pi : \mathbb{R}^3 \rightarrow \mathbb{R}$  be complete sets of eigenstates of the  $\hat{\phi}$  and  $\hat{\pi}$  operators, that is

$$\hat{\phi}(\mathbf{x})|\phi\rangle = \phi(\mathbf{x}) \quad \text{and} \quad \hat{\pi}(\mathbf{x})|\pi\rangle = \pi(\mathbf{x}). \tag{18}$$

Now, we wish to compute the transition amplitude between two field configurations  $\phi$  and  $\phi'$  for a given time difference  $t$ . This is simply  $\langle \phi' | e^{-it\hat{H}} | \phi \rangle$ , however, integrals involving oscillatory terms like this operator are rather difficult to compute. To avoid this computational obstacle, we can replace  $t \rightarrow -it$  which results in the amplitude exhibiting exponential decay instead of oscillation. Doing this doesn't alter any fundamental physics by doing this since the Hamiltonian remains unchanged, but it does change the signature of the spacetime metric from Minkowski to Euclidean. From now on in this thesis, everything from now one will be stated or derived in Euclidean spacetime for continuity. By letting  $N > 0$  be an integer and  $a = t/N$ , we can split the time evolution into  $N$  steps and insert a complete set of field eigenstates to the left of every operator except the leftmost one (since  $\phi'$  is already there) and momentum eigenstates to the right of every operator.

$$\begin{aligned}
\langle \phi' | e^{-t\hat{H}} | \phi \rangle &= \langle \phi' | e^{-a\hat{H}} \cdots e^{-a\hat{H}} | \phi \rangle \\
&= \int \prod_{k=1}^{N-1} d[\phi_k] \int \prod_{l=1}^N d[\pi_l] \langle \phi_N | e^{-a\hat{H}} | \pi_N \rangle \langle \pi_N | \phi_{N-1} \rangle \cdots \langle \phi_1 | e^{-a\hat{H}} | \pi_1 \rangle \langle \pi_1 | \phi_0 \rangle
\end{aligned} \tag{19}$$

where the  $d[\phi_k]$  and  $d[\pi_l]$  serve to notate the integral over all possible configurations of these fields and we've relabeled  $\phi_N = \phi'$  and  $\phi = \phi_0$  for ease of notation. Now we restrict our attention to just one of these operator expectation values in (19). For any  $1 \leq k \leq N$ , since  $H$  is a function of the  $\pi$  and  $\phi$ , the inner product  $\langle \phi_k | e^{-a\hat{H}} | \pi_k \rangle$  for  $a \rightarrow 0$  simply evaluates  $H$  at the field configurations given

$$\begin{aligned}
\langle \phi_k | e^{-a\hat{H}} | \pi_k \rangle &= \langle \phi_k | \mathbb{1} - a\hat{H} | \pi_k \rangle \\
&= (\mathbb{1} - aH(\phi_k, \pi_k)) \langle \phi_k | \pi_k \rangle \\
&= \exp(-aH(\phi_k, \pi_k)) \langle \phi_k | \pi_k \rangle \\
&= \exp\left(\int d^3 \mathbf{x} [-a\mathcal{H}(\phi_k(\mathbf{x}), \pi_k(\mathbf{x})) + i\phi_k(\mathbf{x})\pi_k(\mathbf{x})]\right)
\end{aligned} \tag{20}$$

where we've used the fact that

$$\langle \phi | \pi \rangle = \exp \left( i \int d\mathbf{x} \phi(\mathbf{x}) \pi(\mathbf{x}) \right). \quad (21)$$

Substituting (20) into (19) as well as using (21) to simplify the remaining inner products, we arrive at the formula

$$\begin{aligned} \langle \phi' | e^{-t\hat{H}} | \phi \rangle &= \int \prod_{k=1}^{N-1} d[\phi_k] \int \prod_{l=1}^N d[\pi_l] \\ &\times \exp \left( - \sum_{m=1}^N a \int d^3\mathbf{x} \left[ \mathcal{H}(\phi_m(\mathbf{x}), \pi_m(\mathbf{x})) - i\pi_m(\mathbf{x}) \frac{\phi_m(\mathbf{x}) - \phi_{m-1}(\mathbf{x})}{a} \right] \right). \end{aligned} \quad (22)$$

Letting  $N \rightarrow \infty$ , the first two integrals become integrals over all  $t$ -parametrized paths for  $\pi$  and those of  $\phi$  which satisfy the condition  $\phi(\mathbf{x}, 0) = \phi(\mathbf{x})$  and  $\phi(\mathbf{x}, t) = \phi'(\mathbf{x})$ . The sum in the exponential becomes an integral and the finite difference a derivative. We notate this

$$\begin{aligned} \langle \phi' | e^{-t\hat{H}} | \phi \rangle &= \int_{\phi}^{\phi'} \mathcal{D}[\phi] \int \mathcal{D}[\pi] \\ &\times \exp \left( - \int_0^t dt' \int d^3\mathbf{x} [\mathcal{H}(\phi(\mathbf{x}, t'), \pi(\mathbf{x}, t')) - i\pi(\mathbf{x}, t') \partial_{t'} \phi(\mathbf{x}, t')] \right). \end{aligned} \quad (23)$$

Thus, using (3), we see that (23) becomes

$$\begin{aligned} \langle \phi' | e^{-t\hat{H}} | \phi \rangle &= \int_{\phi}^{\phi'} \mathcal{D}[\phi] \exp \left( - \int_0^t dt' \int d^3\mathbf{x} \left[ \frac{1}{2} \|\nabla \phi(\mathbf{x}, t')\|^2 + \frac{1}{2} m^2 \phi^2(\mathbf{x}, t') \right] \right) \\ &\times \int \mathcal{D}[\pi] \exp \left( - \int_0^t dt' \int d^3\mathbf{x} \left[ \frac{1}{2} \pi^2(\mathbf{x}, t') - i\pi(\mathbf{x}, t') \partial_{t'} \phi(\mathbf{x}, t') \right] \right) \\ &= \int_{\phi}^{\phi'} \mathcal{D}[\phi] \exp \left( - \int_0^t dt' \int d^3\mathbf{x} \left[ \frac{1}{2} (\partial_{t'} \phi(\mathbf{x}, t'))^2 + \frac{1}{2} \|\nabla \phi(\mathbf{x}, t')\|^2 + \frac{1}{2} m^2 \phi^2(\mathbf{x}, t') \right] \right) \\ &\times \int \mathcal{D}[\pi] \exp \left( - \int_0^t dt' \int d^3\mathbf{x} \frac{1}{2} [\pi(\mathbf{x}, t') - i\partial_{t'} \phi(\mathbf{x}, t')]^2 \right) \end{aligned} \quad (24)$$

$$= \int_{\phi}^{\phi'} \mathcal{D}[\phi] \exp(-S_E(\phi)) \quad (25)$$

where we define our path integrals so that the standard Gaussian integrates to one. The  $\pi$  path integral in (24) disappears and the Euclidean action  $S_E$  is

$$S_E(\phi) = \int d^4x \left[ \frac{1}{2} (\partial_t \phi(x))^2 + \frac{1}{2} \|\nabla \phi(x)\|^2 + \frac{1}{2} m^2 \phi^2(x) \right]. \quad (26)$$

The path integral formula for the transition amplitude (25) can also be used to find a path integral formula for the two-point correlation function

$$\langle \phi(\mathbf{x}, t) \phi(0, 0) \rangle = \left\langle 0 \left| e^{t\hat{H}} \phi(\mathbf{x}) e^{-t\hat{H}} \phi(0) \right| 0 \right\rangle. \quad (27)$$

Using a complete basis of energy eigenstates  $|n\rangle$  and the fact that  $e^{-TE_n}$  vanishes in the limit  $T \rightarrow \infty$  for every  $n \neq 0$ , we can rewrite (27) as

$$\begin{aligned}
\langle \phi(\mathbf{x}, t)\phi(0, 0) \rangle &= \lim_{T \rightarrow \infty} \frac{\sum_n e^{-TE_n} \langle n | e^{t\hat{H}} \phi(\mathbf{x}) e^{-t\hat{H}} \phi(0) | n \rangle}{\sum_n e^{-TE_n}} \\
&= \lim_{T \rightarrow \infty} \frac{\sum_{n,m} e^{-TE_n} \langle n | m \rangle \langle m | e^{t\hat{H}} \phi(\mathbf{x}) e^{-t\hat{H}} \phi(0) | n \rangle}{\sum_n e^{-TE_n} \langle n | n \rangle} \\
&= \lim_{T \rightarrow \infty} \frac{\sum_{n,m} \langle n | e^{-T\hat{H}} | m \rangle \langle m | e^{t\hat{H}} \phi(\mathbf{x}) e^{-t\hat{H}} \phi(0) | n \rangle}{\sum_n \langle n | e^{-T\hat{H}} | n \rangle} \\
&= \lim_{T \rightarrow \infty} \frac{\sum_n \langle n | e^{-T\hat{H}} \mathbb{1} e^{t\hat{H}} \phi(\mathbf{x}) e^{-t\hat{H}} \phi(0) | n \rangle}{\sum_n \langle n | e^{-T\hat{H}} | n \rangle} \\
&= \lim_{T \rightarrow \infty} \frac{\text{Tr} \left[ e^{-(T-t)\hat{H}} \phi(\mathbf{x}) e^{-t\hat{H}} \phi(0) \right]}{\text{Tr} \left[ e^{-T\hat{H}} \right]}. \tag{28}
\end{aligned}$$

Now, computing the trace instead with a complete basis of field eigenstates, we get

$$\begin{aligned}
\langle \phi(\mathbf{x}, t)\phi(0, 0) \rangle &= \lim_{T \rightarrow \infty} \frac{\int d[\phi] \langle \phi | e^{-(T-t)\hat{H}} \phi(\mathbf{x}) e^{-t\hat{H}} \phi(0) | \phi \rangle}{\int d[\phi] \langle \phi | e^{-T\hat{H}} | \phi \rangle} \\
&= \lim_{T \rightarrow \infty} \frac{\int d[\phi] \int d[\phi'] \langle \phi | e^{-(T-t)\hat{H}} | \phi' \rangle \langle \phi' | \phi(\mathbf{x}) e^{-t\hat{H}} \phi(0) | \phi \rangle}{\int d[\phi] \langle \phi | e^{-T\hat{H}} | \phi \rangle} \\
&= \lim_{T \rightarrow \infty} \frac{\int d[\phi] \int d[\phi'] \langle \phi | e^{-(T-t)\hat{H}} | \phi' \rangle \langle \phi' | \phi(\mathbf{x}) e^{-t\hat{H}} \phi(0) | \phi \rangle}{\int d[\phi] \langle \phi | e^{-T\hat{H}} | \phi \rangle} \\
&= \lim_{T \rightarrow \infty} \frac{\int d[\phi] \int d[\phi'] \phi'(\mathbf{x})\phi(0) \langle \phi | e^{-(T-t)\hat{H}} | \phi' \rangle \langle \phi' | e^{-t\hat{H}} | \phi \rangle}{\int d[\phi] \langle \phi | e^{-T\hat{H}} | \phi \rangle}. \tag{29}
\end{aligned}$$

Focusing on the numerator of (29),

$$\langle \phi | e^{-(T-t)\hat{H}} | \phi' \rangle = \int_{\phi'}^{\phi} \mathcal{D}[\phi] \exp(-S_E(\phi)) \quad \text{and} \quad \langle \phi' | e^{-t\hat{H}} | \phi \rangle = \int_{\phi}^{\phi'} \mathcal{D}[\phi] \exp(-S_E(\phi))$$

where the first path integral is over a time interval of length  $T - t$  and the second is over  $t$ . Together, they integrate over all paths from  $\phi'$  to itself over an interval length of  $T$  that attain  $\phi$  at time  $t$ . The  $d[\phi]$  integral then integrates over all possible  $\phi$  values, resulting in a path integral over all paths from  $\phi'$  to itself. Lastly, the  $d[\phi']$  integral integrates over all possible values of  $\phi'$  and so the whole numerator is a path integral over all configurations subject to the symmetric time boundary condition  $\phi(\mathbf{x}, 0) = \phi(\mathbf{x}, T)$ . An analysis of the denominator gives a similar result. We can notate this answer as

$$\langle \phi(\mathbf{x}, t)\phi(0, 0) \rangle = \lim_{T \rightarrow \infty} \frac{\int \mathcal{D}[\phi] \phi(\mathbf{x}, t)\phi(0, 0) \exp(-S_E(\phi))}{\int \mathcal{D}[\phi] \exp(-S_E(\phi))} \quad \text{where} \quad \phi(\mathbf{x}, 0) = \phi(\mathbf{x}, T). \tag{30}$$

Carrying out the same process *mutatis mutandis* for a general  $n$ -point correlation function, we see this result generalizes nicely

$$\langle \phi(x_n) \cdots \phi(x_1) \rangle = \lim_{T \rightarrow \infty} \frac{\int \mathcal{D}[\phi] \phi(x_n) \cdots \phi(x_1) \exp(-S_E(\phi))}{\int \mathcal{D}[\phi] \exp(-S_E(\phi))} \quad \text{where} \quad \phi(\mathbf{x}, 0) = \phi(\mathbf{x}, T). \tag{31}$$



### 3 Quantum Chromodynamics

As we are interested in computing properties of the  $B$  meson, we will need to develop the quantum field theory of quarks and the strong force, known as quantum chromodynamics. The material in this section was also heavily sourced from [3].

#### 3.1 Dirac Equation

As quarks are spin-1/2 particles, they are described by the Dirac equation. This has the Lagrangian

$$\mathcal{L}_{\text{Dirac}} = \bar{\psi}_\alpha \left( i\gamma_{\alpha\beta}^\mu \partial_\mu - m\delta_{\alpha\beta} \right) \psi_\beta \quad (32)$$

where  $\psi$  is the four component complex-valued field known as a Dirac spinor,  $\gamma^\mu$  are  $4 \times 4$  matrices that satisfy the anti-commutation relations for Euclidean spacetime

$$\{\gamma^\mu, \gamma^\nu\} = 2\delta^{\mu\nu} \mathbb{1} \quad (33)$$

and  $\bar{\psi}_\alpha = i\psi_\beta^\dagger \gamma_{\beta\alpha}^0$ . There are in general many sets of matrices that satisfy (33), the good news is they are all unitarily equivalent. This means that picking a specific representation won't affect our computations, so we take the Weyl convention

$$\gamma^0 = \begin{bmatrix} 0 & 0 & i & 0 \\ 0 & 0 & 0 & i \\ i & 0 & 0 & 0 \\ 0 & i & 0 & 0 \end{bmatrix} \quad \gamma^1 = \begin{bmatrix} 0 & 0 & 0 & 1 \\ 0 & 0 & 1 & 0 \\ 0 & -1 & 0 & 0 \\ -1 & 0 & 0 & 0 \end{bmatrix} \quad \gamma^2 = \begin{bmatrix} 0 & 0 & 0 & -i \\ 0 & 0 & i & 0 \\ 0 & i & 0 & 0 \\ -i & 0 & 0 & 0 \end{bmatrix} \quad \gamma^3 = \begin{bmatrix} 0 & 0 & 1 & 0 \\ 0 & 0 & 0 & -1 \\ -1 & 0 & 0 & 0 \\ 0 & 1 & 0 & 0 \end{bmatrix}. \quad (34)$$

The conjugate momentum is  $i\bar{\psi}_\alpha \gamma_{\alpha\beta}^0$  and so the Dirac Hamiltonian can be computed as

$$H_{\text{Dirac}} = \int d^3\mathbf{x} \bar{\psi}_\alpha(\mathbf{x}) \left( -i\gamma_{\alpha\beta}^j \partial_j + m\delta_{\alpha\beta} \right) \psi_\beta(\mathbf{x}). \quad (35)$$

When quantizing the field theory, we impose canonical anti-commutation relations on the Dirac spinors since they are Fermionic fields

$$\{\bar{\psi}_\alpha(\mathbf{x}), \psi_\beta(\mathbf{y})\} = \gamma_{\alpha\beta}^0 \delta(\mathbf{x} - \mathbf{y}). \quad (36)$$

With a similar technique to that demonstrated in section 2.2, one can derive the path integral formulas for  $n$ -point correlation functions given by

$$\begin{aligned} & \langle \psi_{\alpha_1}(x_1) \cdots \psi_{\alpha_n}(x_n) \bar{\psi}_{\beta_1}(y_1) \cdots \bar{\psi}_{\beta_n}(y_n) \rangle \\ &= \lim_{T \rightarrow \infty} \frac{\int \mathcal{D}[\bar{\psi}, \psi] \psi_{\alpha_1}(x_1) \cdots \psi_{\alpha_n}(x_n) \bar{\psi}_{\beta_1}(y_1) \cdots \bar{\psi}_{\beta_n}(y_n) \exp(-S_E(\bar{\psi}, \psi))}{\int \mathcal{D}[\bar{\psi}, \psi] \exp(-S_E(\bar{\psi}, \psi))} \end{aligned} \quad (37)$$

where the fields  $\psi$  and  $\bar{\psi}$  are Grassmann-valued, the paths are subject to the anti-symmetric boundary conditions

$$\psi_\alpha(\mathbf{x}, 0) = -\psi_\alpha(\mathbf{x}, T) \quad \text{and} \quad \bar{\psi}_\beta(\mathbf{x}, 0) = -\bar{\psi}_\beta(\mathbf{x}, T) \quad (38)$$

and the Euclidean action is given by

$$S_E(\bar{\psi}, \psi) = \int dx \bar{\psi}_\alpha(x) \left( -i\gamma_{\alpha\beta}^\mu \partial_\mu + m\delta_{\alpha\beta} \right) \psi_\beta(x). \quad (39)$$

#### 3.2 Quantum Chromodynamics and the Lattice

The Dirac Lagrangian alone describes a single non-interacting field. In order to build hadrons with quantum field theory, we will need six quark fields, one for each quark flavor of nature, and a new index for the color charge of the quarks which facilitates their interaction with the gluon field that mediates the strong force. Color charge functions in the theory as the strong analogue of electric charge, however, it has three possible

“signs” which interplay in a fashion similar to additive color, hence the name color charge. The three color charges of quarks are labeled as red, green and blue while anti-quarks carry anti-colors anti-red, anti-green and anti-blue which are often compared to cyan, magenta and yellow respectively. Gluons carry a color and an anti-color and have eight total possible superpositions of pairings. Upon absorption, gluons alter the color content of a quark or anti-quark. The strong interaction also exhibits the property known as *color confinement* which can be surmised as the net color of a system, taken as the addition of the colors under an additive color scheme, must be colorless, i.e. white. This means hadrons, the bound states of quarks, must also be colorless. To describe the color charge mathematically, we introduce another index on the quark field that iterates over one, two and three. From now on, we use early-alphabet Latin characters (e.g.  $a, b, c, \dots$ ) for color indices, early-alphabet Greek characters (e.g.  $\alpha, \beta, \gamma, \dots$ ) for Dirac indices and late-alphabet Greek characters (e.g.  $\mu, \nu, \rho, \dots$ ) for spacetime indices to avoid confusion. The quantum field theory of the strong interaction is known as quantum chromodynamics (QCD) and has the Lagrangian

$$\mathcal{L}_{QCD} = \sum_{\psi \in \{u, d, c, s, t, b\}} \bar{\psi}_{\alpha a} (i\gamma_{\alpha\beta}^{\mu} D_{\mu} - m_{\psi} \delta_{\alpha\beta}) \psi_{\beta a} - \frac{1}{2} G_{\mu\nu}^a G_a^{\mu\nu} \quad (40)$$

where  $\psi$  iterates over the six quark flavors: up, down, top, bottom, strange and charm;  $D_{\mu} = \partial_{\mu} + igA_{\mu}$  is the gauge covariant derivative with  $g$  being the coupling constant of the quark to the gluon field and  $G_a^{\mu\nu}$  is the gluonic field tensor. A general expression for the  $n$ -point correlation function for the interacting theory looks very similar to (37) but with the path integrals taking place over and the Euclidean action depending on all the quark fields and the gluon gauge field  $U$ . Because gluons carry color charge as well, the gluon field self interacts leading to the strongly coupled nature of QCD. This means analytical solutions to the path integral over the gauge fields are not a viable option. Because of this, we turn towards computational techniques and discretize a finite volume of spacetime into a hypercubic lattice  $\Gamma$ . The quark fields then exists on the lattice points and the gluon gauge field on the links between the lattice sites. The action has the general form of

$$S_E(b_{\alpha_b}, \bar{b}_{\beta_b}, \dots, s_{\alpha_s}, \bar{s}_{\beta_s}, U) = \sum_{\psi \in \{u, d, c, s, t, b\}} \sum_{x, y \in \Gamma} \bar{\psi}_{\beta b}(y) K_{\beta\alpha b a}(y, x, U) \psi_{\alpha a}(x) + S_E^{\text{glu}}(U). \quad (41)$$

Where the  $K$  matrices are the discrete versions of the Dirac operator and the remaining terms in the action which only depend on the gauge field we call  $S_E^{\text{glu}}(U)$ . While we discuss QCD in generality, it may be useful to keep in mind that typically in lattice computations only the up, down, strange and sometimes charm quarks are included as sea quarks, i.e. only these quarks’ terms are included in the sum over  $\psi$  in (41). Theses quarks, being the lightest, have the most significant contributions due to virtual pair production and therefore must be included as sea quarks. From the form of (41), we see that when computing  $n$ -point correlation functions, we can split the path integrals over the different quark fields and gauge field. As it turns out, the path integrals over the quark fields have nice analytical solutions which we discuss in the next section.

### 3.2.1 Generating Functional and Contractions for the Dirac Field

As it turns out, the path integral over a Dirac field in the  $n$ -point correlation function not only has a nice analytical result, but it can be written down very quickly just by following a few rules known as contractions. We’ll first introduce the generating functional which is a rigorous mathematical way of computing these path integrals and then show how it gives rise to the rules of contractions. For now we restrict to just one Dirac field but the solution will generalize easily. We define the generating functional for the Dirac field as

$$Z(\bar{\eta}, \eta) = \int \mathcal{D}[\bar{\psi}, \psi] \exp \left( -S_E(\bar{\psi}, \psi) + \sum_{x, y \in \Gamma} \bar{\eta}_{\alpha}(x) \psi_{\alpha}(x) + \bar{\psi}_{\alpha}(x) \eta_{\alpha}(x) \right) \quad (42)$$

where  $\eta$  and  $\bar{\eta}$  are arbitrary Dirac fields. The  $S_E$  here is the lattice Dirac action

$$S_E(\bar{\psi}, \psi) = \sum_{x, y \in \Gamma} \bar{\psi}_{\beta}(y) K_{\beta\alpha}(y, x) \psi_{\alpha}(x) \quad (43)$$

where this  $K$  matrix is the lattice Dirac operator. It can be shown through the properties of Grassmann integration that this integral has an analytical formula

$$Z(\bar{\eta}, \eta) = \det K \exp \left( \sum_{x, y \in \Gamma} \left[ \bar{\eta}_{\alpha a}(x) K_{\alpha \beta ab}^{-1}(x, y) \eta_{\beta b}(y) \right] \right) \quad (44)$$

where the determinant and inverses are taken over spacetime coordinates, Dirac indices and color indices.  $K_{-1}$  in the context of QCD is known as the quark propagator. We can then see from (42) and the properties of Grassmann differentiation that we can rewrite the  $n$ -point correlation function as

$$\begin{aligned} & \langle \psi_{\alpha_1}(x_1) \cdots \psi_{\alpha_n}(x_n) \bar{\psi}_{\beta_1}(y_1) \cdots \bar{\psi}_{\beta_n}(y_n) \rangle \\ &= \frac{(-1)^n}{Z(0, 0)} \frac{\partial}{\partial \bar{\eta}_{\alpha_1}(x_1)} \cdots \frac{\partial}{\partial \bar{\eta}_{\alpha_n}(x_n)} \frac{\partial}{\partial \eta_{\beta_1}(y_1)} \cdots \frac{\partial}{\partial \eta_{\beta_n}(y_n)} Z(\bar{\eta}, \eta) \Big|_{\eta = \bar{\eta} = 0}. \end{aligned} \quad (45)$$

Now, since we have a nice analytic formula for  $Z(\bar{\eta}, \eta)$ , we can take these derivatives explicitly. From the properties of Grassmann variables, we can show this becomes

$$\begin{aligned} & \langle \psi_{\alpha_1}(x_1) \cdots \psi_{\alpha_n}(x_n) \bar{\psi}_{\beta_1}(y_1) \cdots \bar{\psi}_{\beta_n}(y_n) \rangle \\ &= (-1)^{\frac{n(n-1)}{2}} \sum_{\sigma \in S_n} \text{sign}(\sigma) K_{\alpha_1 \beta_{\sigma(1)}}^{-1}(x_1, y_{\sigma(1)}) \cdots K_{\alpha_n \beta_{\sigma(n)}}^{-1}(x_n, y_{\sigma(n)}). \end{aligned} \quad (46)$$

We notice this formula can be generated by a quick algorithm on the symbols of the  $n$ -point correlation function: for a possible set of pairs of  $\psi$ 's and  $\bar{\psi}$ 's, we anti-commute keeping track of the sign until each of the pairs are beside each other with the  $\psi$  on the left, then replace these pairs with the corresponding  $K^{-1}$ , then sum over all possible pairings. This is what's known as the contraction algorithm and it makes computing  $n$ -point correlation functions of the Dirac field incredibly quick and easy to do. This same algorithm applies in the full QCD interacting picture as well with the added rule that only fields of like-quark flavors can contract together. This means we can analytically reduce all of the quark field path integrals in a full QCD  $n$ -point correlation function analytically, but we still have to commute the path integral over the gauge field. Unfortunately, this can not be done analytically and so we must turn to computational methods to solve this.

### 3.2.2 Computationally Solving the Gauge Field Path Integral

In a full QCD  $n$ -point correlation function, the contractions eliminate the path integrals; however, since the Dirac operators now include the gauge covariant derivative (41), the contractions are dependent on the gauge field  $U$ . A general expression for an  $n$ -point correlation function can then be expressed as

$$\langle \cdots \rangle = \frac{\int \mathcal{D}[U] (\text{contractions of } \cdots) \left( \prod_{\psi} \det K_{\psi}(U) \right) \exp \left( -S_E^{\text{glu}}(U) \right)}{\int \mathcal{D}[U] \left( \prod_{\psi} \det K_{\psi}(U) \right) \exp \left( -S_E^{\text{glu}}(U) \right)} \quad (47)$$

On the lattice, this path integral becomes discretized into a multi-dimensional integral over the gauge field values at all the links in the lattice. To evaluate this integral, we define the gauge field probability distribution as

$$P(U) \propto \left( \prod_{\psi} \det K_{\psi}(U) \right) \exp \left( -S_E^{\text{glu}}(U) \right). \quad (48)$$

Then, we can rearrange the integrals in (47) to give

$$\begin{aligned} \langle \cdots \rangle &= \int \mathcal{D}[U] (\text{contractions of } \cdots) \frac{\left( \prod_{\psi} \det K_{\psi}(U) \right) \exp \left( -S_E^{\text{glu}}(U) \right)}{\int \mathcal{D}[U] \left( \prod_{\psi} \det K_{\psi}(U) \right) \exp \left( -S_E^{\text{glu}}(U) \right)} \\ &= \int \mathcal{D}[U] (\text{contractions of } \cdots) P(U) \\ &= \langle \text{contractions of } \cdots \rangle_U \end{aligned}$$

where  $\langle \cdot \rangle_U$  here notates the expectation value over the gauge field probability distribution. Therefore, by generating a sample set of gauge field configurations  $\{U_i\}_{i=1}^N$  with probability  $P(U)$ , we can evaluate the integral by computing the average of the contractions over this sample set.

## 4 Electromagnetic Form Factor of the $B$ Meson

Electromagnetic form factors find their roots in scattering theory as an analogue for charge distribution of a target. We reproduce the quantum mechanical derivation here and then define the  $b$  quark contribution to the form factor of the  $B$  meson and compute it using two and three-point correlation function lattice computations.

### 4.1 Electromagnetic Form Factors

For a scattering interaction between a stationary target with potential  $V_{\text{int}}$  that dies off at large distance and a particle with incoming wave function  $\psi_i$  and outgoing wave function  $\psi_f$  far from the target, the Born approximation gives a scattering cross section which depends on the matrix element  $|\langle \psi_f | V_{\text{int}} | \psi_i \rangle|^2$  [5]. We expect that  $\psi_i$  and  $\psi_f$  are plane waves with momenta  $\mathbf{p}$  and  $\mathbf{p}'$  respectively and under the assumption that the dominating interaction between the particle and the target is electromagnetism, then the potential is given by  $V_{\text{int}} = q_p \phi(\mathbf{x})$  where  $\phi$  is the electric potential of the target and  $q_p$  is the electric charge of the scattered particle. This allows us to evaluate the matrix element as

$$\begin{aligned} \langle \psi_f | V_{\text{int}} | \psi_i \rangle &= \int d^3\mathbf{x} e^{-i\mathbf{x}\cdot\mathbf{p}'} q_p \phi(\mathbf{x}) e^{i\mathbf{x}\cdot\mathbf{p}} \\ &= -\frac{q_p}{\|\mathbf{p} - \mathbf{p}'\|^2} \int d^3\mathbf{x} \phi(\mathbf{x}) \Delta e^{i\mathbf{x}\cdot(\mathbf{p}-\mathbf{p}')} \\ &= -\frac{q_p}{\|\mathbf{p} - \mathbf{p}'\|^2} \int d^3\mathbf{x} \left[ \Delta \left( \phi(\mathbf{x}) e^{i\mathbf{x}\cdot(\mathbf{p}-\mathbf{p}')} \right) - e^{i\mathbf{x}\cdot(\mathbf{p}-\mathbf{p}')} \Delta \phi(\mathbf{x}) \right]. \end{aligned} \quad (49)$$

Letting  $\mathbf{q} = \mathbf{p} - \mathbf{p}'$  be the momentum transfer, using the divergence theorem and the assumption that  $\phi$  dies off quick enough, the integral over the first term in (49) gives zero. Using Gauss' equation, we can write the second term in terms of the charge density  $\rho(\mathbf{x})$  giving

$$\langle \psi_f | V_{\text{int}} | \psi_i \rangle = -\frac{q_p}{\epsilon_0 \|\mathbf{q}\|^2} \int d^3\mathbf{x} \rho(\mathbf{x}) e^{i\mathbf{x}\cdot\mathbf{q}}. \quad (50)$$

It is the integral expression in (50) that we define as the electric form factor of the target

$$F(\mathbf{q}) = \int d^3\mathbf{x} \rho(\mathbf{x}) e^{i\mathbf{x}\cdot\mathbf{q}}. \quad (51)$$

The form factor, as the inverse Fourier transform of the charge distribution of the target, encodes all of the information needed to reconstruct said charge distribution of the target. The charge distribution of the  $B$  meson is expected to be spherically symmetric so the form factor can only depend on  $\|\mathbf{q}\|$ . Now we wish to find a Taylor expansion around  $\|\mathbf{q}\| = 0$  and we'll compute the first three terms here.

$$\begin{aligned} F(0) &= \int d^3\mathbf{x} \rho(\mathbf{x}) \\ &= Q_{\text{tot}} \end{aligned} \quad (52)$$

where  $Q_{\text{tot}}$  is the total charge of the target. Next,

$$\begin{aligned}
\left. \frac{d}{d|\mathbf{q}|} F(|\mathbf{q}|) \right|_{|\mathbf{q}|=0} &= \left. \frac{d}{d|\mathbf{q}|} \int d^3\mathbf{x} \rho(\mathbf{x}) e^{i|\mathbf{x}|\cdot|\mathbf{q}| \cos(\theta)} \right|_{|\mathbf{q}|=0} \\
&= i \int d^3\mathbf{x} |\mathbf{x}| \cos(\theta) \rho(\mathbf{x}) \\
&= 2\pi i \int_0^\pi d\theta \cos(\theta) \sin(\theta) \int_0^\infty dr r^3 \rho(r) \\
&= 0.
\end{aligned} \tag{53}$$

This is because cosine is an odd function while sine is an even one on the interval 0 to  $\pi$ . Lastly,

$$\begin{aligned}
\left. \frac{d^2}{d^2|\mathbf{q}|} F(|\mathbf{q}|) \right|_{|\mathbf{q}|=0} &= \left. \frac{d^2}{d^2|\mathbf{q}|} \int d^3\mathbf{x} \rho(\mathbf{x}) e^{i|\mathbf{x}|\cdot|\mathbf{q}| \cos(\theta)} \right|_{|\mathbf{q}|=0} \\
&= -\frac{1}{3} \int_0^\infty 4\pi r^2 dr r^2 \rho(r) \\
&= -\frac{1}{3} Q_{\text{tot}} \langle r^2 \rangle
\end{aligned} \tag{54}$$

where  $\langle r^2 \rangle$  is the average squared charge radius. We see that, in general, the odd derivatives will vanish and that the form factor will only depend on  $|\mathbf{q}|^2$ . This result is true for the quantum field theory framework as well, giving

$$F(Q^2) = Q_{\text{tot}} \left( 1 - \frac{1}{6} \langle r^2 \rangle Q^2 + \dots \right) \tag{55}$$

where  $Q^2 = -q^\mu q_\mu$  is the space-like square of the momentum transfer. Fitting the form factor with a line in  $Q^2$  then allows us to easily compute the root mean square charge radius  $r_{\text{RMS}} = \sqrt{\langle r^2 \rangle}$  from the slope.

## 4.2 Computational Setup

We use an identical lattice setup to the ‘‘C005’’ ensemble in [6] with a quarter of the gauge field configuration samples. The lattice has 24 sites in each spatial direction and 64 in the temporal direction. The up and down quark masses are both set equal to  $0.005/a$  where  $a$  is the lattice spacing  $0.1106(3)$  fm as determined in [7]. We use non-relativistic quantum chromodynamics (NRQCD) [8] for the lattice action of the bottom quark and the fully relativistic domain-wall action [9, 10, 11, 12] for the up, down and strange quarks. We quench the charm, top and bottom quark fields in our computations, i.e. set the determinant of the corresponding propagators in (47) to one. Although these determinants will have a non-zero contribution to the correlation functions due to virtual pair production, we expect their contributions to be significantly smaller due to their large masses.

## 4.3 The $B$ Meson Form Factor

The  $B^+$  meson, which we refer to just as the  $B$  meson from now on, has bottomness +1, upness +1 and  $J^P = 0^-$ . We define the form factor of the  $B$  meson  $F_B(Q^2)$  as

$$\langle B(\mathbf{p}) | J^\mu(\mathbf{0}) | B(\mathbf{p}') \rangle = (p + p')^\mu F_B(Q^2) \tag{56}$$

where  $J_\mu$  is the electromagnetic four-current and  $|B(p)\rangle$  is the pure  $B$  meson state, the lowest energy state with momentum  $p$  and the quantum numbers listed above. Because we cannot analytically compute this state, we must define  $B$  meson interpolating fields which have the same quantum numbers as the  $B$  meson and project them onto the desired momentum state. We give these interpolating fields and the  $b$  quark contribution to the electromagnetic four-current as

$$\phi_B(x) = \bar{u}_{\alpha\alpha}^{\text{sm}}(x) (\gamma^5)_{\alpha\beta} b_{\beta a}(x), \tag{57a}$$

$$\phi_B^\dagger(x) = -\bar{b}_{\alpha a}(x) (\gamma^5)_{\alpha\beta} u_{\beta\alpha}^{\text{sm}}(x), \tag{57b}$$

$$J^\mu(x) = \bar{b}_{\alpha a}(x) (\gamma^\mu)_{\alpha\beta} b_{\beta a}(x). \tag{57c}$$

where  $\gamma^5 = i\gamma^0\gamma^1\gamma^2\gamma^3$  and  $u^{sm}$  is the smeared up-quark field defined as

$$u^{sm} = \left(1 + \frac{\sigma\Delta}{4N}\right)^N u. \quad (58)$$

where we use  $N = 30$  and  $\sigma = 4.350$  with  $\Delta$  being the gauge covariant Laplacian on the lattice. Acting with the interpolating field on the vacuum state  $\phi_B^\dagger(x)|0\rangle$  stimulates the  $B$  meson state as well as many other higher energy states which we call contamination states. Time evolving this state results in each of the contributions exponentially decaying as  $e^{-Et}$  where  $E$  is the energy of the state. All of the contributions by the contamination states will be exponentially suppressed relative to that of the  $B$  meson after long enough time. Thus, any quantity computed with the interpolating field approaches that of the  $B$  meson at large time. Because it is expected that the up quark, being the lighter of the two, will be more de-localized in the  $B$  meson, smearing the up quark operators removes some of the contamination states' contributions to  $\phi_B^\dagger(x)|0\rangle$ , forcing faster convergence to the  $B$  meson state.

#### 4.3.1 Two-Point and Three-Point Correlation Functions for the $B$ Meson

To compute the  $B$  meson form factor according to (56), we will need to compute some two and three-point correlation functions and then project them to a specific momentum. For notational clarity, we reintroduce the quark propagators as

$$G_{\alpha\beta ab}^u(\mathbf{x}, t_1^{sm}, \mathbf{y}, t_2^{sm}) = \langle u_{\alpha a}^{sm}(\mathbf{x}, t_1) \bar{u}_{\beta b}^{sm}(\mathbf{y}, t_2) \rangle, \quad (59)$$

$$G_{\alpha\beta ab}^b(\mathbf{x}, t_1, \mathbf{y}, t_2) = \langle b_{\alpha a}^{sm}(\mathbf{x}, t_1) \bar{b}_{\beta b}(\mathbf{y}, t_2) \rangle \quad (60)$$

which obey  $\gamma^5$ -hermiticity

$$G_{\alpha\beta ab}^{u\dagger}(\mathbf{x}, t_1^{sm}, \mathbf{y}, t_2^{sm}) = \gamma^5 G_{\alpha\beta ab}^u(\mathbf{x}, t_1^{sm}, \mathbf{y}, t_2^{sm}) \gamma^5, \quad (61)$$

$$G_{\alpha\beta ab}^{b\dagger}(\mathbf{x}, t_1, \mathbf{y}, t_2) = \gamma^5 G_{\alpha\beta ab}^b(\mathbf{x}, t_1, \mathbf{y}, t_2) \gamma^5. \quad (62)$$

Now we define the  $B$  meson two-point correlation function as

$$\begin{aligned} C_{2pt}(\mathbf{p}, t) &= \sum_{\mathbf{x}} \langle \phi_B(\mathbf{x}, t) \phi_B^\dagger(0, 0) \rangle e^{-i\mathbf{p}\cdot\mathbf{x}} \\ &= - \sum_{\mathbf{x}} \langle \bar{u}_{\alpha a}^{sm}(\mathbf{x}, t) (\gamma^5)_{\alpha\beta} b_{\beta a}(\mathbf{x}, t) \bar{b}_{\delta b}(0, 0) (\gamma^5)_{\delta\epsilon} u_{\epsilon b}^{sm}(0, 0) \rangle e^{-i\mathbf{p}\cdot\mathbf{x}} \\ &= \sum_{\mathbf{x}} \langle (\gamma^5)_{\delta\epsilon} u_{\epsilon b}^{sm}(0, 0) \bar{u}_{\alpha a}^{sm}(\mathbf{x}, t) (\gamma^5)_{\alpha\beta} b_{\beta a}(\mathbf{x}, t) \bar{b}_{\delta b}(0, 0) \rangle e^{-i\mathbf{p}\cdot\mathbf{x}} \\ &= \sum_{\mathbf{x}} (\gamma^5)_{\delta\epsilon} G_{\epsilon\alpha ba}^u(0, 0^{sm}, \mathbf{x}, t^{sm}) (\gamma^5)_{\alpha\beta} G_{\beta\delta ab}^b(\mathbf{x}, t, 0, 0) e^{-i\mathbf{p}\cdot\mathbf{x}} \\ &= \sum_{\mathbf{x}} G_{\delta\beta ba}^{u\dagger}(0, 0^{sm}, \mathbf{x}, t^{sm}) G_{\beta\delta ab}^b(\mathbf{x}, t, 0, 0) e^{-i\mathbf{p}\cdot\mathbf{x}} \\ &= \sum_{\mathbf{x}} \text{Tr} [G^{u\dagger}(0, 0^{sm}, \mathbf{x}, t^{sm}) G^b(\mathbf{x}, t, 0, 0)] e^{-i\mathbf{p}\cdot\mathbf{x}} \end{aligned} \quad (63)$$

where here we've only evaluated the path integral over the quark fields and have left off the gauge field integral to prevent the notation from becoming too cluttered.

We define the three-point correlation function as

$$\begin{aligned}
C_{3\text{pt}}^\mu(\mathbf{p}, \mathbf{p}', t, \tau) &= \sum_{\mathbf{x}, \mathbf{y}} \left\langle \phi_B(\mathbf{y}, t) J^\mu(\mathbf{x}, \tau) \phi_B^\dagger(0, 0) \right\rangle e^{-i\mathbf{p}\cdot\mathbf{x} - i\mathbf{p}'\cdot(\mathbf{y}-\mathbf{x})} \\
&= - \sum_{\mathbf{x}, \mathbf{y}} \left\langle \bar{u}_{\alpha a}^{\text{sm}}(\mathbf{y}, t) (\gamma^5)_{\alpha\beta} b_{\beta a}(\mathbf{y}, t) \bar{b}_{\delta b}(\mathbf{x}, \tau) (\gamma^\mu)_{\delta\epsilon} b_{\epsilon b}(\mathbf{x}, \tau) \bar{b}_{\zeta c}(0, 0) (\gamma^5)_{\zeta\eta} u_{\eta c}^{\text{sm}}(0, 0) \right\rangle e^{-i\mathbf{p}\cdot\mathbf{x} - i\mathbf{p}'\cdot(\mathbf{y}-\mathbf{x})} \\
&= \sum_{\mathbf{x}, \mathbf{y}} \left[ (\gamma^5)_{\zeta\eta} G_{\eta\alpha ca}^u(0, 0^{\text{sm}}, \mathbf{y}, t^{\text{sm}}) (\gamma^5)_{\alpha\beta} G_{\beta\delta ab}^b(\mathbf{y}, t, \mathbf{x}, \tau) (\gamma^\mu)_{\delta\epsilon} G_{\epsilon\zeta bc}^b(\mathbf{x}, \tau, 0, 0) \right. \\
&\quad \left. - (\gamma^5)_{\zeta\eta} G_{\eta\alpha ca}^u(0, 0^{\text{sm}}, \mathbf{y}, t^{\text{sm}}) (\gamma^5)_{\alpha\beta} G_{\epsilon\delta bb}^b(\mathbf{x}, \tau, \mathbf{x}, \tau) (\gamma^\mu)_{\delta\epsilon} G_{\beta\zeta ac}^b(\mathbf{y}, t, 0, 0) \right] e^{-i\mathbf{p}\cdot\mathbf{x} - i\mathbf{p}'\cdot(\mathbf{y}-\mathbf{x})} \\
&= \sum_{\mathbf{x}, \mathbf{y}} \left[ \text{Tr} \left[ G^{u\dagger}(0, 0^{\text{sm}}, \mathbf{y}, t^{\text{sm}}) G^b(\mathbf{y}, t, \mathbf{x}, \tau) \gamma^\mu G^b(\mathbf{x}, \tau, 0, 0) \right] \right. \\
&\quad \left. - \text{Tr} \left[ G^{u\dagger}(0, 0^{\text{sm}}, \mathbf{y}, t^{\text{sm}}) G^b(\mathbf{y}, t, 0, 0) \right] \text{Tr} \left[ G^b(\mathbf{x}, \tau, \mathbf{x}, \tau) \gamma^\mu \right] \right] e^{-i\mathbf{p}\cdot\mathbf{x} - i\mathbf{p}'\cdot(\mathbf{y}-\mathbf{x})}. \tag{64}
\end{aligned}$$

The second term in (64) is said to be disconnected and is expected to be small compared to the connected term so we neglect it and define the three-point correlation function as

$$C_{3\text{pt}}^\mu(\mathbf{p}, \mathbf{p}', t, \tau) = \sum_{\mathbf{x}, \mathbf{y}} \text{Tr} \left[ G^{u\dagger}(0, 0^{\text{sm}}, \mathbf{y}, t^{\text{sm}}) G^b(\mathbf{y}, t, \mathbf{x}, \tau) \gamma^\mu G^b(\mathbf{x}, \tau, 0, 0) \right] e^{-i\mathbf{p}\cdot\mathbf{x} - i\mathbf{p}'\cdot(\mathbf{y}-\mathbf{x})}. \tag{65}$$

Again, we've notationally left off the gauge field path integral that we must still carry out. In the large  $t$  and  $\tau$  limits, we expect these expressions to well-approximate

$$C_{2\text{pt}}(\mathbf{p}, t) \approx \frac{A_B^2}{2E_B(\mathbf{p})} e^{-E_B(\mathbf{p})t} \tag{66}$$

and

$$C_{3\text{pt}}^\mu(\mathbf{p}, \mathbf{p}', t, \tau) \approx \frac{A_B^2}{4E_B(\mathbf{p}')E_B(\mathbf{p})} \langle B(\mathbf{p}') | J^\mu(\mathbf{0}) | B(\mathbf{p}) \rangle e^{-E_B(\mathbf{p}')(t-\tau) - E_B(\mathbf{p})\tau} \tag{67}$$

where  $A_B$  is the unknown amplitude of the  $B$  meson excited by the state  $\phi_B^\dagger(x) | 0 \rangle$ . To extract the form factor from these correlation functions, we use the method outlined in [13] and define the ratio  $R^\mu(\mathbf{p}, \mathbf{p}', t, \tau)$  as

$$R^\mu(\mathbf{p}, \mathbf{p}', t, \tau) = \frac{C_{3\text{pt}}^\mu(\mathbf{p}, \mathbf{p}', t, \tau)}{\sqrt{C_{2\text{pt}}(\mathbf{p}, t) C_{2\text{pt}}(\mathbf{p}', t)}} \sqrt{\frac{C_{2\text{pt}}(\mathbf{p}, t-\tau) C_{2\text{pt}}(\mathbf{p}', \tau)}{C_{2\text{pt}}(\mathbf{p}', t-\tau) C_{2\text{pt}}(\mathbf{p}, \tau)}}. \tag{68}$$

It then follows from (66) and (67) that

$$\lim_{\substack{t \rightarrow \infty \\ \tau \rightarrow \infty}} R^\mu(\mathbf{p}, \mathbf{p}', t, \tau) = \langle B(\mathbf{p}') | J^\mu(\mathbf{0}) | B(\mathbf{p}) \rangle. \tag{69}$$

From here, we use the time component of (56) to compute the form factor,

$$F_B(Q^2) = \frac{1}{E(\mathbf{p}) + E(\mathbf{p}')} \lim_{\substack{t \rightarrow \infty \\ \tau \rightarrow \infty}} R^0(\mathbf{p}, \mathbf{p}', t, \tau) \tag{70}$$

where  $Q^2 = -q^\mu q_\mu = -(p - p')^\mu (p - p')_\mu$  is the space-like square of the momentum transfer.

## 4.4 Results

For our gauge field sample set we used 77 gauge configurations made available by the RBC and UKQCD collaborations [14]. On each configuration, the contribution to the two and three-point correlation functions were computed for one 'exact' run and 32 'sloppy' runs. In the exact run, the quark propagators were solved to a relative precision of  $10^{-8}$ . In the sloppy runs, the propagators were solved less precisely and the gauge field configuration was randomly translated. We introduce  $C_{2\text{pt}}^{is}(\mathbf{p}, t)$  and  $C_{3\text{pt}}^{\mu, is}(\mathbf{p}, \mathbf{p}', t, \tau)$  as notations for these contributions to the two and three-point correlation functions where the index  $i = 1, \dots, 77$  notates

the gauge configuration and the index  $s = 0, \dots, 32$  notates the run-type with  $s = 0$  corresponding to the exact run and  $s = 1, \dots, 32$  being the sloppy runs. The  $s = 1$  run is the sloppy run with zero translation. The data were then averaged over the run-type index according to

$$C_{2\text{pt}}^i(\mathbf{p}, t) = C_{2\text{pt}}^{i0}(\mathbf{p}, t) - C_{2\text{pt}}^{i1}(\mathbf{p}, t) + \frac{1}{32} \sum_{s=1}^{32} C_{2\text{pt}}^{is}(\mathbf{p}, t) \quad (71)$$

$$C_{3\text{pt}}^{\mu,i}(\mathbf{p}, \mathbf{p}', t, \tau) = C_{3\text{pt}}^{\mu,i0}(\mathbf{p}, \mathbf{p}', t, \tau) - C_{3\text{pt}}^{\mu,i1}(\mathbf{p}, \mathbf{p}', t, \tau) + \frac{1}{32} \sum_{s=1}^{32} C_{3\text{pt}}^{\mu,is}(\mathbf{p}, \mathbf{p}', t, \tau). \quad (72)$$

This averaging was chosen to ensure the expectation value of  $C_{2\text{pt}}^i(\mathbf{p}, t)$  and  $C_{3\text{pt}}^{\mu,i}(\mathbf{p}, \mathbf{p}', t, \tau)$  were the same as that of the exact runs. Then, computing the path integral over the gauge fields boils down to taking the average of these over the configuration index  $i$ . Due to the non-relativistic treatment of the  $b$  quark, the energies of the states all receive a constant shift [8]. This means to compute the energies in (70) correctly, we must determine the kinetic mass of the  $B$  meson, defined as

$$m_{\text{kin}} = \frac{\|\mathbf{p}\|^2 - (E_B(\mathbf{p}) - E_B(\mathbf{0}))^2}{2(E_B(\mathbf{p}) - E_B(\mathbf{0}))} \quad (73)$$

where these energies are extracted by fitting exponentials in time to the two-point correlation functions at these momentum values. The energies in (70) are then computed using the kinetic mass according to

$$E(\mathbf{p}) = \sqrt{\|\mathbf{p}\|^2 + m_{\text{kin}}^2}. \quad (74)$$

We chose  $\mathbf{p}/a = (2\pi/24, 0, 0)$  and the fits were done from  $t/a = 7$  to  $t/a = 22$  as this regime was determined to minimize excited state contamination, which dominates at early time, and minimize noise from the finite size of the lattice, which dominates at late time. The uncertainty in this result was computed using a bootstrapping method by removing configurations from the sample set and fitting for the energies. The results are plotted in Figure 1 and the calculated result according to (73) was determined to be

$$am_{\text{kin}} = 3.00 \pm 0.43.$$

This agrees with the value computed with the ‘‘C005’’ ensemble in [6]. Since their value  $am_{\text{kin}} = 3.002(40)$  was computed more precisely, we use it in our determination of the form factor instead.

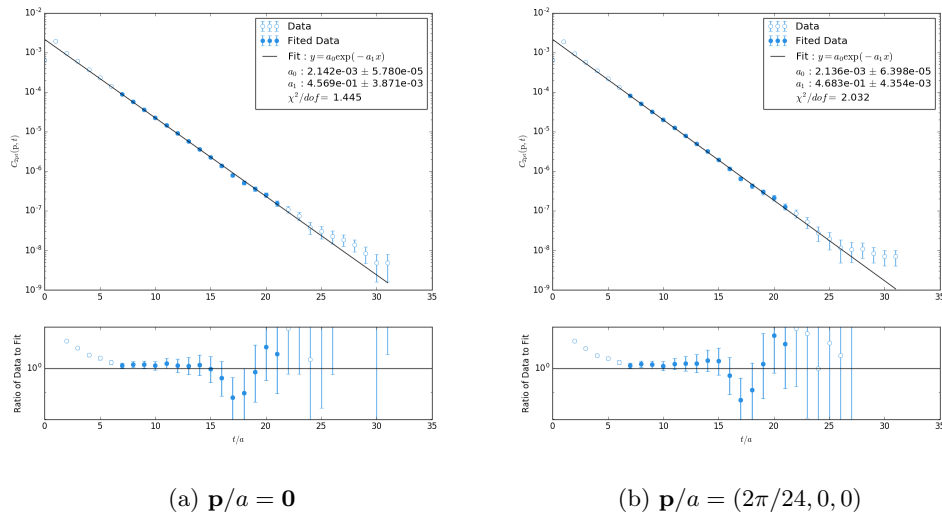


Figure 1: Unbiased two-point correlation functions for two  $\mathbf{p}$  values fitted from  $t/a = 7$  to  $t/a = 22$ .



The form factor was computed via (70) for each gauge field configuration by first computing  $R^0(\mathbf{p}, \mathbf{p}', t, \tau)$  from the unbiased data according to (68). The form factor for each configuration was then normalized so that  $F_B(0) = 1$ . From these, the expected form factor and uncertainties were computed using a bootstrap method for three different choices of symmetric-time current insertion:  $(\tau, t) = (4, 8), (6, 12), (8, 16)$ . The form factors were then plotted over  $Q^2$  and fit with a line to extract the root mean square of the charge radius according to (55). These results are shown in Figure 2 and Table 1.

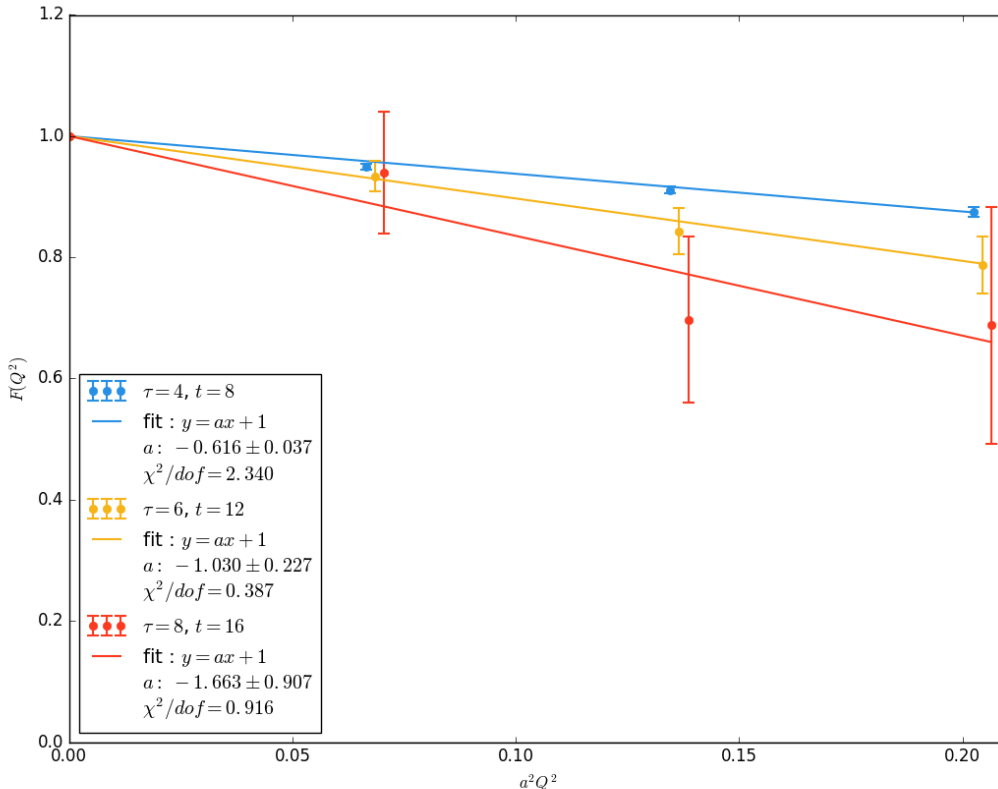


Figure 2: The  $B$  meson form factor with data taken for three different choices of time. The data points are slightly staggered for clarity.

$\tau/a$	$t/a$	$r_{\text{RMS}}/a$	$r_{\text{RMS}}$ (fm)
4	8	$1.922 \pm 0.057$	$0.2125 \pm 0.0063$
6	12	$2.48 \pm 0.27$	$0.274 \pm 0.30$
8	16	$3.16 \pm 0.86$	$0.349 \pm 0.95$

Table 1: Root mean square of bottom-quark charge radius computed from form factor.

As the times gradually increase, the  $r_{\text{RMS}}$  values change. This is because for small time, the correlation functions are dominated by the contamination states. We expect for large enough time, the computed values will stabilize as the contribution from the contamination states becomes exponentially suppressed and so we take  $r_{\text{RMS}} = 0.349 \pm 0.95$  fm to be our most reliable value.

## 5 Outlook

The form factor and  $r_{\text{RMS}}$  value reported are most likely not free from systematic error. As we only computed the form factor for three time-values, we were unable to confirm any convergence of the form factor for large time. Even though we saw convergence of the two-point correlation function for time values on this interval, it is still possible that the contamination states influence the form factor at this time scale. An obvious next step would be computing the form factor for more  $Q^2$  values and more symmetric-time current insertions to better constrain each charge radius value and to be able to see the convergence occur. Moving forward, we could also include the up quark current contribution which we left out for ease of computation. This would likely lead to a larger value for the charge radius as the up quark is much lighter than the bottom quark, so we expect it is much more de-localized in the meson. Going beyond the  $B$  meson, another interesting hadron just recently shown to be stable is the doubly-bottom  $\bar{b}bud$  tetraquark [6]. The techniques applied in this thesis, in addition to the techniques applied by Leskovec et al., could be translated easily to a computation of the tetraquark's electromagnetic form factor. This would give us more insight, beyond just its mass, into the internal structure of the tetraquark.

## References

- [1] G. Elor, M. Escudero, and A. Nelson, “Baryogenesis and Dark Matter from  $B$  Mesons,” *Phys. Rev.* **D99** no. 3, (2019) 035031, [arXiv:1810.00880 \[hep-ph\]](#).
- [2] C.-W. Hwang, “Charge radii of light and heavy mesons,” *Eur. Phys. J.* **C23** (2002) 585–590, [arXiv:hep-ph/0112237 \[hep-ph\]](#).
- [3] S. Meinel, *Heavy quark physics on the lattice with improved nonrelativistic actions*. PhD thesis, 2010.
- [4] M. E. Peskin and D. V. Schroeder, *An Introduction to quantum field theory*. Addison-Wesley, Reading, USA, 1995.
- [5] B. Povh, *Particles and nuclei: an introduction to the physical concepts*. Springer, 1999.
- [6] L. Leskovec, S. Meinel, M. Pflaumer, and M. Wagner, “Lattice QCD investigation of a doubly-bottom  $\bar{b}bud$  tetraquark with quantum numbers  $I(J^P) = 0(1^+)$ ,” [arXiv:1904.04197 \[hep-lat\]](#).
- [7] **RBC, UKQCD** Collaboration, T. Blum *et al.*, “Domain wall QCD with physical quark masses,” *Phys. Rev.* **D93** no. 7, (2016) 074505, [arXiv:1411.7017 \[hep-lat\]](#).
- [8] G. P. Lepage, L. Magnea, C. Nakhleh, U. Magnea, and K. Hornbostel, “Improved nonrelativistic QCD for heavy quark physics,” *Phys. Rev.* **D46** (1992) 4052–4067, [arXiv:hep-lat/9205007 \[hep-lat\]](#).
- [9] D. B. Kaplan, “A Method for simulating chiral fermions on the lattice,” *Phys. Lett.* **B288** (1992) 342–347, [arXiv:hep-lat/9206013 \[hep-lat\]](#).
- [10] V. Furman and Y. Shamir, “Axial symmetries in lattice QCD with Kaplan fermions,” *Nucl. Phys.* **B439** (1995) 54–78, [arXiv:hep-lat/9405004 \[hep-lat\]](#).
- [11] Y. Shamir, “Chiral fermions from lattice boundaries,” *Nucl. Phys.* **B406** (1993) 90–106, [arXiv:hep-lat/9303005 \[hep-lat\]](#).
- [12] R. C. Brower, H. Neff, and K. Orginos, “The Möbius domain wall fermion algorithm,” *Comput. Phys. Commun.* **220** (2017) 1–19, [arXiv:1206.5214 \[hep-lat\]](#).
- [13] N. Hasan, J. Green, S. Meinel, M. Engelhardt, S. Krieg, J. Negele, A. Pochinsky, and S. Syritsyn, “Computing the nucleon charge and axial radii directly at  $q^2 = 0$  in lattice qcd,” [arXiv:1711.11385](#).
- [14] **RBC, UKQCD** Collaboration, Y. Aoki *et al.*, “Continuum Limit Physics from 2+1 Flavor Domain Wall QCD,” *Phys. Rev.* **D83** (2011) 074508, [arXiv:1011.0892 \[hep-lat\]](#).